10 September 2026

Semicrystalline Polyesters Made by Stereoselective Polymerization of a Biobased Bicyclic Lactone

David M. Dumas[1], Kai Hin Lui[1], Hongyi Zhang[1], Matthew W. Kanan[1], Robert M. Waymouth[1]

1. Department of Chemistry, Stanford University

Abstract

Biobased thermoplastics offer sustainable alternatives to petrochemical plastics, but controlling polymer stereochemistry to access biobased materials with desirable thermomechanical properties remains a challenge. Here, we report two new semicrystalline thermoplastics synthesized through the stereoselective ring-opening polymerization of the biobased bicyclic lactone (±)-2-oxo-3,8dioxabicyclo[3.2.1]octane (ODO). Enantiopure bisurea catalysts produced highly syndiotactic poly(ODO) (s-PODO) at low temperatures through an unexpected chain-end control mechanism. Yttrium-catalyzed melt polymerizations afforded high-molecular weight isotactic and syndiotactic PODO. The ductility, strength and modulus of PODO thermoplastics can be tuned through changes in tacticity, processing and crystallinity. By controlling their stereoregularity and processing conditions, we show that semicrystalline PODO films can have exceptional gas barrier properties with enhanced strength and modulus relative to amorphous atactic PODO.

Semicrystalline Polyesters Made by Stereoselective Polymerization of a Biobased Bicyclic Lactone

David M. Dumas[1]†, Kai Hin Lui[1]†, Hongyi Zhang[1]†, Matthew W. Kanan[1]*, Robert M. Waymouth[1]*

[1]Department of Chemistry, Stanford University; 337 Campus Drive, Stanford, California, 94305, United States

*Corresponding author. Email: waymouth@stanford.edu, mkanan@stanford.edu

†These authors contributed equally to this work.

Biobased thermoplastics offer sustainable alternatives to petrochemical plastics, but controlling polymer stereochemistry to access biobased materials with desirable thermomechanical properties remains a challenge. Here, we report two new semicrystalline thermoplastics synthesized through the stereoselective ring-opening polymerization of the biobased bicyclic lactone (±)-2-oxo-3,8-dioxabicyclo[3.2.1]octane (ODO). Enantiopure bisurea catalysts produced highly syndiotactic poly(ODO) (*s*-PODO) at low temperatures through an unexpected chain-end control mechanism. Yttrium-catalyzed melt polymerizations afforded high-molecular weight isotactic and syndiotactic PODO. The ductility, strength and modulus of PODO thermoplastics can be tuned through changes in tacticity, processing and crystallinity. By controlling their stereoregularity and processing conditions, we show that semicrystalline PODO films can have exceptional gas barrier properties with enhanced strength and modulus relative to amorphous atactic PODO.

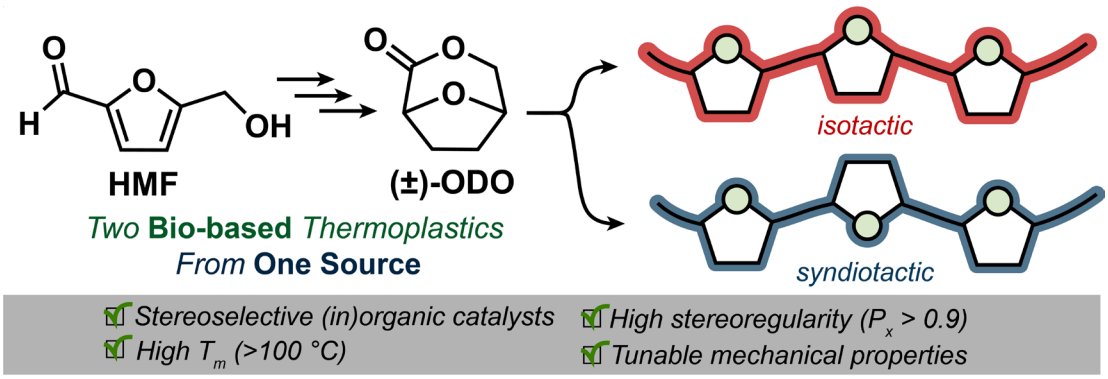

Introduction

Beneficial physical properties, tunability, and low cost have propelled the exponential growth of petrochemical plastics over the past several decades (*1, 2*). However, rising alarm about the enormous volumes of persistent plastic pollution and the growing resource intensity of plastic production have motivated the development of biobased plastics as potentially more sustainable alternatives (*3-5*). In addition to being renewable, biomass offers access to monomers that are infeasible to produce from petrochemical feedstocks, which can be leveraged to achieve property advantages. Polyesters figure prominently among existing biobased plastics, and examples such as poly(lactic acid) (PLA) and poly(hydroxyalkanoates) (PHAs) have gained traction because they provide alternative end-of-life options such as industrial composting (*6*). Compared to petroleum-based commodity thermoplastics, however, biobased polyesters typically have inferior physical properties, which limit their competitiveness (*2*).

For aliphatic polyesters that contain stereogenic centers in the backbone, the polymer tacticity – the stereochemical configuration of sequential monomers in the polymer chains – can have a substantial influence on its crystallinity and thermomechanical properties (*7*). Controlling polyester tacticity by stereoselective ring-opening polymerization (ROP) is well-established for monocyclic monomers such as *meso*- and *rac*-lactide (*8-13*), *rac*-β-butyrolactone (*14, 15*) and its *rac*-diolide derivatives (*16, 17*), *rac*-alkyl-β-malolactonates (*18*), and *rac*-*O*-carboxyanhydrides (*19-21*). Bicyclic lactone monomers have recently received increased attention because polyesters derived from these monomers incorporate cyclic structures in the repeating unit that can impart improved thermomechanical properties and facilitate chemical recycling (*22-30*). In contrast to monocyclic monomers, stereoselective ROP is not well established for bicyclic lactones, with a few recent examples of stereoselective ROP of petroleum-based bicyclic lactones (*30, 31*).

Herein we describe two new stereoregular crystalline thermoplastics derived from racemic (±)-2-oxo-3,8-dioxabicyclo[3.2.1]octane ((±)-ODO), a bridged bicyclic lactone accessible from the 6-carbon bio-sourced 5-hydroxymethylfurfural (HMF). We had previously reported the ring-opening polymerization of racemic ODO to generate amorphous atactic (*a*-PODO) and the copolymerization of ODO with L-lactide to generate more ductile PLA (*22*). As described below, the stereoselective ring-opening polymerization of racemic (±)-ODO by new classes of organic bisurea or Yttrium-based catalysts provide access to stereoregular, semi-crystalline thermoplastics derived from erythro-di-isotactic PODO (isotactic, *i*-PODO) and erythro-di-syndiotactic PODO (syndiotactic, *s*-PODO). We report the surprising discovery that chiral bisurea organocatalysts (*32, 33*) can produce syndiotactic PODO by a chain-end control mechanism (*34*), supported through polymerization and kinetic modeling of these chiral catalysts with enantiopure and racemic ODO. Syndio- and isoselective yttrium catalyst mixtures were also developed to produce high-molecular weight samples. The resulting polymers are distinct semi-crystalline materials that exhibit tacticity- and processing-dependent thermal, mechanical, and gas barrier properties.

Results and Discussion

Ring-opening polymerization of ODO with Bisureas

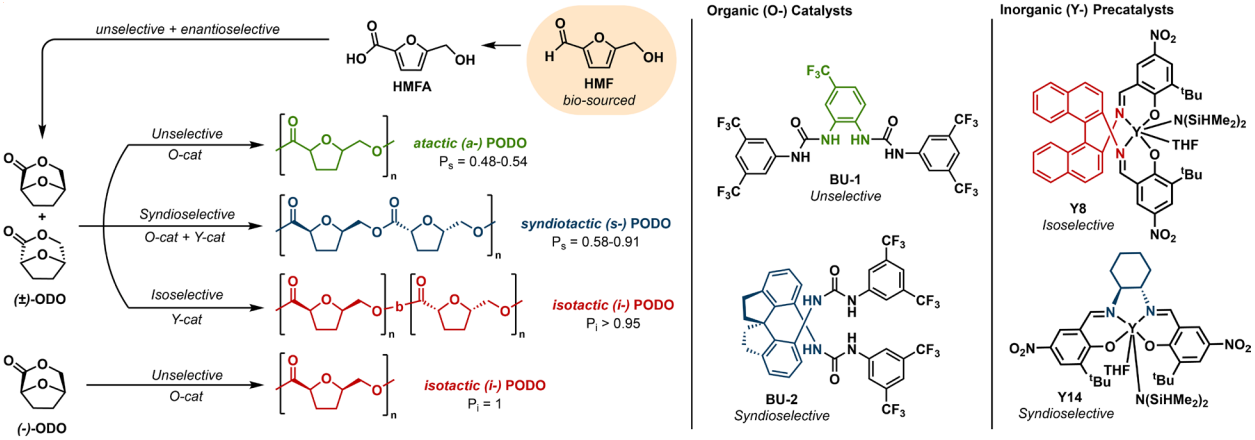

Fig. 1. Reaction scheme for synthesis of ODO and PODO of various tacticities.

We first prepared homochiral *i*-PODO from the ROP of enantiopure ODO to determine whether stereoregular PODO is semicrystalline (Fig. 1). The enantiopure monomer was synthesized through diastereoselective hydrogenation of the chiral amide ***R*-1** derived from 5-(hydroxymethyl)-2-furoic acid and (*R*)-diphenyl(pyrrolidine-2-yl)methanol (*35*). Hydrogenation of ***R*-1** afforded (5-hydroxymethyl)tetrahydrofuran-2-carboxamide ***R*-2** with 86% diastereomeric excess, which could be recrystallized to diastereomerically pure ***R*-2** (Fig. S11). Single crystal X-ray diffraction established its absolute configuration as the (2*S*,5*R*)-HMTA-(*R*)-amide (Fig. S76, Table S6). Hydrolysis of ***R*-2** to the acid, followed by acid-catalyzed lactonization under azeotropic conditions afforded (−)-(1*S*,5*R*)-3,8-dioxabicyclo[3.2.1]-octan-2-one ((−)-(1*S*,5*R*)-ODO) as a colorless crystalline solid (*22*).

Both (±)-ODO and (−)-ODO underwent rapid polymerization at room temperature with deprotonated achiral bisurea, **BU-1** (*32*) (Figure 1), reaching 93% conversion after 3 min (Table S1, entries 8-10). The polymer obtained from (±)-ODO was a transparent viscous solid, whereas the polymerization of (−)-ODO yielded a colorless powder (Fig. 2D). To measure polymer tacticity, the mass quantities of diads in the carbonyl region of the carbon-13 nuclear magnetic resonance (^{13}C-NMR) of PODO were measured. PODO prepared from (±)-ODO displayed two resonances of equal intensity (δ = 172.60 – 172.80 ppm, Fig. 2E), consistent with stereorandom, *a*-PODO (*22*). PODO prepared from (−)-ODO displayed only the more upfield ^{13}C NMR resonance, which we attribute to the isotactic diad of two (2*S*,5*R*)-5-(hydroxymethyl)tetrahydrofuran-2-carboxylate repeat units. ROP of (−)-ODO and (±)-ODO with the strongly basic phosphazene base P2-^{t}Bu afforded PODO with no new resonances, indicating negligible epimerization during ROP (Table S1, entries 24-25).

Homochiral *i*-PODO derived from (−)-(1*S*,5*R*)-ODO is optically active with a molar optical rotation of $[\Phi]^{D}$ of -9.4±1.3° (Table S5, entry 5). Interestingly, methyl (2S,5R)-5-(hydroxymethyl)tetrahydrofuran-2-carboxylate, a model for the repeat unit of *i*-PODO, exhibits a molar optical rotation of the opposite sign ($[\Phi]^{D}$ = +4.3±0.1°, entry 3). The modest difference in optical rotation between the monomer model and the polymer likely indicates a weak preference towards helical polymer conformations in solution (*36-38*).

Differential scanning calorimetry (DSC) and wide-angle powder x-ray diffraction showed that homochiral *i*-PODO is semicrystalline (Fig. 2A, F). These results established that stereoregularity

can confer crystallinity to PODO and motivated the development of catalysts for direct stereoselective polymerization of racemic ODO.

Stereoregular polyesters have been generated from racemic monomers by chain-end and enantiomorphic site control mechanisms (*7*). Because ODO propagates from a primary alcohol chain end and PODO made from (±)-ODO with achiral **BU-1** is atactic, we initially suspected that ODO would not be amenable to stereoselective polymerization by chain-end control. We therefore synthesized and evaluated a library of chiral bisurea organocatalysts (*32, 33*) for the stereoselective polymerization of (±)-ODO (Fig. S1, Table S1). Polymerizations performed with **BU-2** (Fig. 1), a chiral bisurea derived from 2,2',3,3'-tetrahydro-1,1'-spirobi[1H-indene]-7,7'-diamine, exhibited a high rate of polymerization and high stereoselectivity compared to **BU-1**. ROP of (±)-ODO with racemic **BU-2** at room temperature proceeded to 88% conversion in 5 minutes (Table S1, entry 11). ^{13}C NMR of the resulting polymer was enriched in the more downfield carbonyl resonance (Fig. 2E), indicating predominantly erythro-di-syndiotactic PODO (syndiotactic, *s*-PODO, P_s = 0.73) was formed.

Many chiral syndioselective catalysts operate by a polymeryl exchange mechanism, rapidly swapping mismatched chain ends between catalytic centers, which requires the presence of both enantiomers of the catalyst (*12, 39-41*). To probe the origin of syndioselectivity in **BU-2**, we compared the polymerization of (±)-ODO using racemic versus enantiopure catalyst at various temperatures (Table S1, entries 11-22). Surprisingly, both enantiopure and racemic **BU-2** afforded highly *syndiotactic* PODO ($P_s > 0.90$) when run at low temperatures (Table S1, entry 20-22). These results are consistent with a chain-end control mechanism for **BU-2**, where monomer insertion is dictated by the chirality of the active chain end (*30, 41, 42*), an unusual behavior for a chiral catalyst. To the best of our knowledge, **BU-2** is the only organocatalyst that exhibits a syndioselective chain-end control mechanism.

Additional experiments with **(*R*)-BU-2** suggest that the stereoselectivity of this organocatalytic system is sensitive to the choice of non-nucleophilic base, the presence of both urea segments, and the electronics of the phenyl motif (Table S3).

To gain further insights into the mechanism of **BU-2** at low temperatures, the kinetics of (±)-ODO and (−)-ODO ROP were investigated at -72 °C with **BU-2** of various optical purities (Fig. S77). Kinetic experiments closely follow first-order kinetics, with enantiopure, enantioenriched, and racemic **BU-2** exhibiting similar rates for the polymerization of (±)-ODO that are within experimental error. This indicates that polymeryl exchange between catalysts of different chirality is not the dominant syndioselective mechanism. Furthermore, the polymerization rates of (−)-ODO by either **BU-2** enantiomer are much slower than the polymerization rate of (±)-ODO, reinforcing a chain-end control mechanism where the cross-propagation rate is much higher than the homo-propagation rate. Since information on the stereoregularity of the polymer is limited to diad and triad resolution on the ^{13}C NMR (Table S7), we developed a model to supplement these measurements. By adopting a first-order Markov kinetic model and assuming quasi-steady-state on the active chain ends, we show that the syndiotactic propagation rate constants can be uniquely determined from experimentally measured rates (k_{app}) and the syndiotacticity of the resulting polymer (see supp. text). These calculations show that the cross-propagation rates are 5.7 and 43 times that of the homo-propagation rates depending on the chain end.

Thermal and Spectral Analysis of Stereoregular PODO

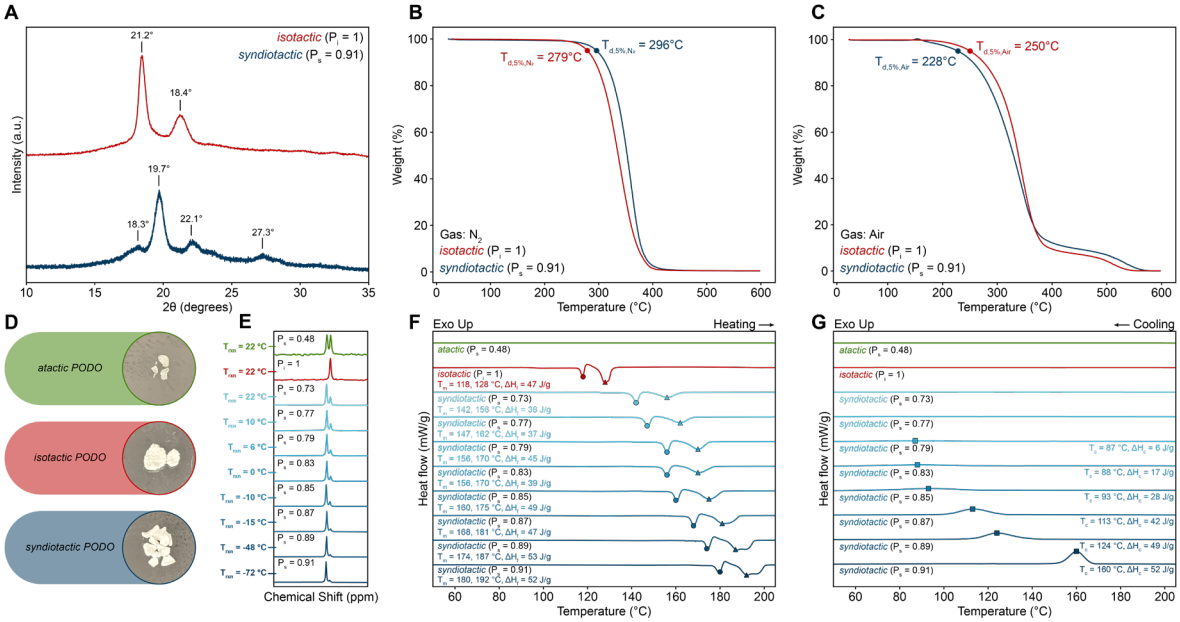

Fig. 2. Diffractive and thermal characterization of low M_w stereoregular PODO from BU-1 and BU-2. (A) pXRD of i-PODO ($P_i > 0.95$) and s-PODO ($P_s = 0.91$). (B) TGA of i-PODO ($P_i > 0.95$) and s-PODO ($P_s = 0.91$) at 10°C/min under N_2. (C) TGA of i-PODO ($P_i > 0.95$) and s-PODO ($P_s = 0.91$) at 10°C/min under air. (D) Images of atactic, isotactic and syndiotactic powder isolated from BU experiments. (E) ^{13}C-NMR of carbonyl resonance of PODO of various tacticities run at various reaction temperatures (T_{rxn}). (F) DSC heating ramp of PODO at 10°C/min. Heating scan shown was taken after samples were annealed at a designated temperature (T_a) from the melt for 3 hours. (G) DSC cooling ramp of PODO at 10°C/min. Cooling scan was taken directly after the heating scan previously shown.

We examined highly stereoregular samples of *i*-PODO ($P_i = 1$) and *s*-PODO ($P_s = 0.91$) with comparable molecular weights (M_n = 10 - 15 kDa) via differential scanning calorimetry (DSC), powder X-ray diffraction (pXRD), and thermogravimetric analysis (TGA) (Fig. 2). Samples subjected to DSC were first annealed from the melt at a temperature (T_a) ~40 °C below their melting temperature (T_m) for 3 hours to allow crystallinity to develop under similar processing conditions (Table S4). DSC of *i*-PODO exhibited two melting endotherms at 118 and 128 °C with a total enthalpy of fusion (ΔH_f) of 47 J/g and no recrystallization exotherm upon cooling (Fig. 2G-F), whereas *s*-PODO ($P_s = 0.91$) exhibited two melting endotherms at 180 °C and 192 °C (ΔH_f = 52 J/g) and a crystallization exotherm at 160 °C (ΔH_c = 52 J/g). Upon cooling from the melt at 10 °C/min, *s*-PODO completely recovered its crystallinity, indicating fast crystallization on the timescale of the DSC ramp. The emergence of distinct X-ray diffraction peaks confirms the crystallinity observed by DSC and suggests that differences in crystalline morphology may contribute to the 60 °C difference in T_m between tacticities. (Fig. 2A). TGA revealed onset decomposition temperatures under N_2 ($T_{d,5\%,N2}$) of 296 °C and 279 °C for *i*-PODO and *s*-PODO, respectively (Fig. 2B), which is 15 °C higher than *a*-PODO ($T_{d,\ 5\%,N2}$ = 262 °C) (*22*). Under air, the onset decomposition temperatures ($T_{d,5\%,air}$) of *i*-PODO and *s*-PODO samples are 250 °C and 228 °C, respectively.

As the T_m of the highly syndiotactic *s*-PODO ($P_s = 0.91$) samples are only 30 °C below the decomposition temperature ($T_{d,5\%,air}$), the window for melt-processing these materials is quite narrow (Fig. 2C, F). To improve *s*-PODO's melt processibility, we generated PODO samples of variable syndiotacticity (P_s = 0.73-0.91) by using different reaction temperatures with **BU-2** (Fig. 2E, Table S1 & S4). The T_m and T_c of *s*-PODO decreased with P_s, indicating that the melting

properties can be tuned by controlling the degree of syndiotacticity (Fig. 2E-G) (*31, 41*). For example, a syndiotactic sample of $P_s = 0.79$ exhibits a T_m of 170 °C and still retains a crystallization endotherm ($T_c = 87$ °C) at 10 °C/min. Given the range of accessible melting behaviors for *s*-PODO, moderately syndiotactic ($P_s \leq 0.8$) materials may be more useful thermoplastics as they have a more than 60 °C processing window.

High Molecular Weight Stereoregular PODO.

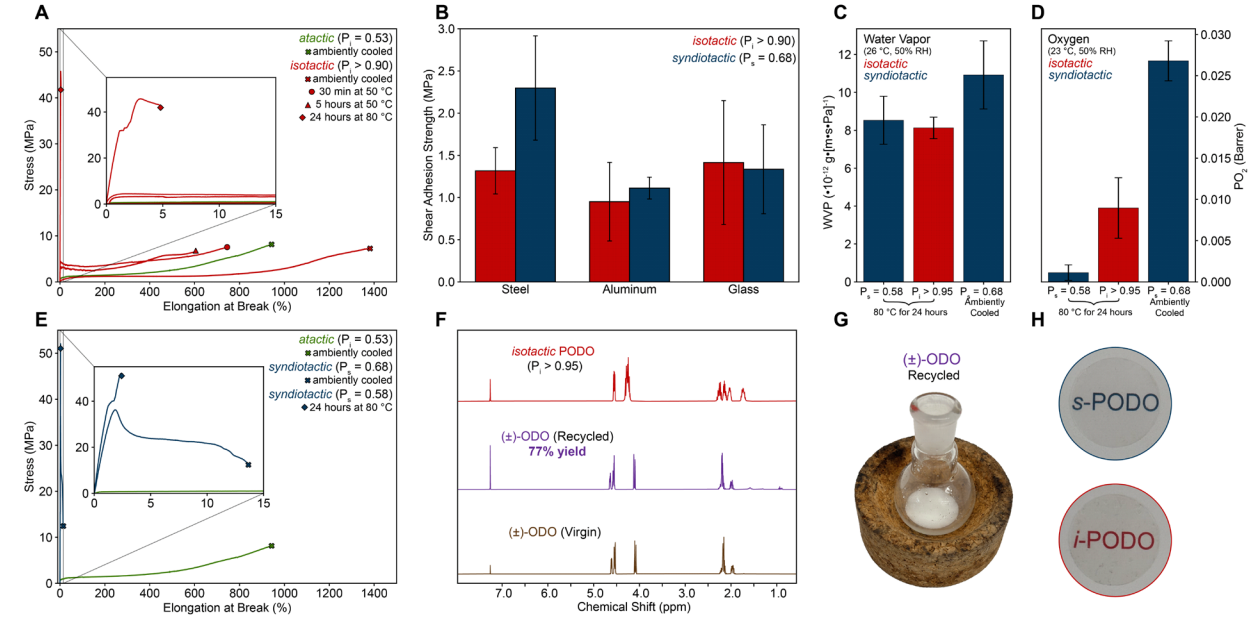

Fig. 3. Material characterization and chemical recovery of high Mw PODO. (A) Uniaxial tensile tests of representative samples of *a*-PODO (M_n = 67.1 kDa, Đ = 2.78, P_i = 0.53) and *i*-PODO (M_n = 43.0 kDa, Đ = 2.12, $P_i > 0.95$) after ambient cooling from the melt and various thermal treatments at 5 mm/min. (B) Lap shear adhesion strength of hot-melted *i*-PODO (M_n = 43.0 kDa, Đ = 2.12, $P_i > 0.95$), and *s*-PODO (M_n = 23.7 kDa, Đ = 3.55, P_s = 0.68) on various inorganic substrates. (C) Water vapor permeability of thermally treated *i*-PODO (M_n = 43.0 kDa, Đ = 2.12, $P_i > 0.95$), and *s*-PODO (M_n = 47.0 kDa, Đ = 2.17, P_s = 0.58) compared to ambiently cooled *s*-PODO (M_n = 23.7 kDa, Đ = 3.55, P_s = 0.68). (D) Oxygen permeability of thermally treated (held for 24 hours at 80°C) *i*-PODO (M_n = 43.0 kDa, Đ = 2.12, $P_i > 0.95$), and *s*-PODO (M_n = 47.0 kDa, Đ = 2.17, P_s = 0.58) compared to ambiently cooled *s*-PODO (M_n = 23.7 kDa, Đ = 3.55, P_s = 0.68). (E) Uniaxial tensile tests of representative samples of *a*-PODO (M_n = 67.1 kDa, Đ = 2.78, P_i = 0.53), *s*-PODO (M_n = 23.7 kDa, Đ = 3.55, P_s = 0.68) and *s*-PODO (M_n = 47.0 kDa, Đ = 2.17, P_s = 0.58) after ambient cooling from the melt and long thermal treatment at 5 mm/min. (F) Chemical recycling of *i*-PODO (M_n = 43.0 kDa, Đ = 2.12, $P_i > 0.95$) to crude (±)-ODO. (G) Image of chemically recycled (±)-ODO. (H) Images of *s*-PODO and *i*-PODO thin films.

The promising thermal properties of the *i*- and *s*-PODO encouraged us to develop metal-based catalysts capable of making high molecular weight stereoregular PODO at room temperature or via melt polymerization. We evaluated a series of yttrium complexes generated *in situ* by combining an appropriate ligand with $Y(N(Si(H)Me_2)_2)_3 \bullet (THF)_2$ (Table S8), a catalyst system previously utilized for the stereoselective polymerization of lactones (*7, 43*). From these screening studies, two promising ligands were identified. A catalyst derived from **rac-L8** produced isotactic-enriched PODO from (±)-ODO under melt polymerization conditions, affording *i*-PODO with $P_i > 0.95$ and molecular weight (M_n) of up to 422 kDa. Under comparable conditions, a catalyst derived from **rac-L14** produced syndiotactic-enriched PODO with P_s between 0.58-0.81 and M_n of up to 372 kDa (Table S9). Differing from the bisurea organocatalysts, these yttrium catalysts exhibit higher rates and can maintain stereoselectivity at 45-60 °C in neat monomer (Table S9). Variations in syndioselecivity were observed with the **rac-L14** derived catalyst during large-scale melt polymerizations (> 3 g), potentially due to uncontrolled heating from the reaction exotherm.

We evaluated the tensile properties of high-molecular weight *a*-, *i*-, and *s*-PODO samples on melt-pressed tensile bars in accordance with the ASTM-D638 standard. *a*-PODO (M_n = 67.1 kDa, Đ = 2.78, P_i = 0.53) exhibited a low modulus (E =1.6±0.3 MPa) and high elongation at break (ε_b = 966.2±152.4%), consistent with previously reported mechanical behavior (Fig. 3A, Table S10-11) (*22*). Tensile specimens of *i*-PODO (M_n = 43.0 kDa, Đ = 2.12, P_i > 0.95) were prepared by ambiently cooling samples from the melt, which resulted in a material that exhibits no clear melting transition (Fig. S79). Ambiently cooled samples of *i*-PODO exhibited high ductility (ε_b = 1505.0 ± 462.0%) and a low modulus (E =113.7±266.2 MPa), similar to *a*-PODO. The absence of clear melting transitions in ambiently cooled *i*- and *a*-PODO by DSC and the similarities in their mechanical behavior (Fig. S78-S79, Table S12, entry 1,3) demonstrate that amorphous PODO samples are elastomeric regardless of stereoregularity. Contrastingly, high molecular weight *s*-PODO materials (M_n = 23.7 kDa, Đ = 3.55, P_s = 0.68) prepared by ambient cooling from the melt were stiff, strong, and relatively brittle (E = 2578.0±321.2 MPa, σ_y = 33.5 ± 4.0 MPa, ε_b = 17.4 ± 14.6%) (Fig. 3E, Table S11, entry 2). Fast crystallization in *s*-PODO renders semicrystalline material under ambient cooling conditions, resulting in thermoplastic mechanical behavior.

Previous annealing experiments on *i*-PODO and *s*-PODO suggest that thermal treatment can modulate crystallinity (Fig. 2F, Table S4). To study the impact annealing may have on the semicrystallinity and mechanical behavior of *i*-PODO, high molecular weight samples were thermally treated at 50 °C for less than 5 hours or at 80 °C for 24 hours. DSC verified a relationship between annealing time and the resulting material's crystallinity (Fig. S79-S84, Table S12). Thermally treated *i*-PODO (M_n = 43.0 kDa, Đ = 2.12, P_i > 0.95) samples exhibited a high modulus >1 GPa, reaching as high as ~3.6 GPa after considerable annealing (Fig. 3E, Table S11, entry 4-6). The ductility of these samples rapidly decreased from > 500% to ~ 6% with increasing thermal treatment, indicating that these materials embrittle as they crystallize. Interestingly, a mildly syndiotactic sample (M_n = 47.0 kDa, Đ = 2.17, P_s = 0.58) can be subjected to a long annealing time and attain a comparably high modulus > 3 GPa (Fig. 3E). This result suggests that the degree of stereoregularity (P_x) required to generate strong materials with a high T_m (> 100 °C) is much lower for syndiotactic samples (Table S11-S12, entry 6-7). The wide variability in modulus, strength and ductility across various processing conditions suggests that the mechanical behavior of stereoregular PODO is closely linked to its crystalline morphology. Since commercial plastics are processed in a variety of ways, having tunable crystallization and melting behaviors may be advantageous.

The lap shear adhesion strength of hot-melted *i*- and *s*-PODO was measured on inorganic substrates in accordance with ASTM D1002 for metal-to-metal adhesion and ASTM C961 for glass-to-glass adhesion. Both *i*-PODO (M_n = 43.0 kDa, Đ = 2.12, P_i > 0.95), and *s*-PODO (M_n = 23.7 kDa, Đ = 3.55, P_s = 0.68) exhibited moderate adhesion strength (1-2 MPa) to steel, aluminum and borosilicate glass substrates after thermal treatment for 24 hours at 80°C (Fig. 2B).

The water vapor and oxygen permeabilities of highly crystalline samples of *i*- and *s*-PODO were measured on melt-pressed films in accordance with ASTM E96 and ASTM 3985, respectively. Highly crystalline samples of *i*-PODO (M_n = 43.0 kDa, Đ = 2.12, P_i > 0.95, ΔH_f = 29 J/g), and s-PODO (M_n = 47.0 kDa, Đ = 2.17, P_s = 0.58, ΔH_f = 29 J/g) prepared by thermal annealing (i.e., held at 80°C for 24 hours), were subject to gas barrier testing alongside an unannealed, moderately syndiotactic (M_n = 23.7 kDa, Đ = 3.55, P_s = 0.68, ΔH_f = 16 J/g) sample of lower crystallinity (Fig. 2C-D, Table S12, entry 2, 6-7). Thermally treated samples of *i*- and *s*-PODO exhibited a low water permeability ($WVP_{i\text{-}PODO} = 8.12 \pm 0.57 \cdot 10^{-12} \cdot g[m \cdot s \cdot Pa]^{-1}$, $WVP_{s\text{-}PODO} = 8.53 \pm 1.27 \cdot 10^{-12} \cdot g[m \cdot s \cdot Pa]^{-1}$) and an extremely low oxygen permeability ($PO_{2,i\text{-}PODO}$ =

$8.95\pm3.77\cdot10^{-3}$ Barrer, $PO_{2,s\text{-}PODO} = 1.12\pm0.94\cdot10^{-3}$ Barrer). An untreated sample of s-PODO (P_s = 0.68) also exhibited comparable water permeability (WVP = $10.92 \pm 1.80\cdot10^{-12}\cdot g[m\cdot s\cdot Pa]^{-1}$) but substantially higher O_2 permeability (PO_2 = $26.8\pm2.4\cdot10^{-3}$ Barrer). Differences in permeability between untreated *s*-PODO (P_s = 0.68) and thermally treated *s*-PODO (P_s = 0.58) suggest that crystallinity and aging behavior are more important factors in attaining low gas permeability than the degree of syndiotacticity.

Chemical recyclability has been previously demonstrated for *a*-PODO, however, we were interested in understanding if stereoregularity impacts recyclability. High molecular weight *i*-PODO (M_n = 43.0 kDa, Đ = 2.12, P_i > 0.95) was heated to 180 °C under vacuum in the presence of $Sn(Oct)_2$ and glycerol ethoxylate (GEO, M_n = 1 kDa). Within hours, (±)-ODO was reactively distilled from *i*-PODO in high yield (77% yield, Fig. 3F-G).

In comparing stereoregular PODO to the thermal, mechanical and barrier performance of other commercial plastics, we see that PODO stands out as a promising new biobased thermoplastic. The melting temperatures of stereoregular PODO lie well above 100 °C and are comparable to commercial plastics like high-density poly(ethylene) (HDPE), poly(lactic acid) (PLA), poly(hydroxybutyrate) (PHB) and poly(propylene) (PP) (Fig. 4A) (*2*). In its highly crystalline form, stereoregular PODO can behave like a high modulus (E > 2 GPa), high strength (σ_y > 40 MPa) material comparable to PLA and PHB (Fig. 4B, Table S11, S17) (*2*). With minimal processing, isotactic PODO is a high elongation (ε_b > 500%) material with comparable modulus to HDPE (E ~ 1 GPa). Lastly, highly crystalline samples of stereoregular PODO exhibit exceptionally low oxygen permeabilities comparable to poly(ethylene terephthalate) (PET) and PHB, while retaining water vapor permeabilities lower than common bioplastics like PLA and poly(butylene-adipate-co-terephthalate) (PBAT) (Fig. 4B) (*2, 44-46*).

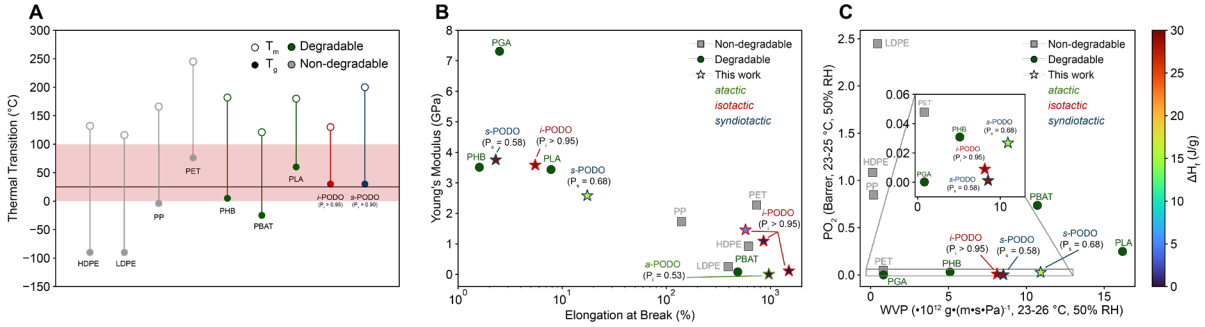

Fig. 4. Comparison of PODO's material properties to commercial plastics. (A) Comparison of i-PODO (P_i > 0.95) and s-PODO's (P_s = 0.91) thermal properties to other commercial plastics compiled from ref. (*2*). (B) Comparison of *i*-PODO (P_i > 0.95) and *s*-PODO's (P_s = 0.58-0.68) mechanical properties to other commercial plastics compiled from ref. (*2*). (C) Comparison of *i*-PODO (P_i > 0.95) and *s*-PODO's (P_s = 0.58-0.68) water vapor and oxygen barrier properties to other commercial plastics compiled from ref. (*2, 44-46*).

Conclusions

As new bicyclic lactones continue to emerge, methods of stereoselective catalysis are needed to access semicrystalline polyesters with exceptional thermal and mechanical properties. We present two new biobased semicrystalline polyesters accessed through the stereoselective polymerization of a racemic bicyclic lactone, ODO, using two different catalysts systems. We demonstrate that syndioselectivity in our chiral bisureas arise through chain-end control, an unusual mode of stereocontrol for an enantiopure organocatalyst. We also reveal two yttrium catalysts that are iso- and syndioselective, capable of accessing high molecular weight materials (M_n up to 422 kDa) with high stereoregularity (P_i > 0.95, P_s = 0.58-0.81).

Stereoregularity can be tuned by decreasing the reaction temperature, which can increase the melting temperature (T_m) of *s*-PODO over a 50 °C range. Thermal analysis of *s*-PODO reveals that *s*-PODO has a higher T_m and an observable T_c compared to *i*-PODO made from enantiopure (−)-ODO. Variation in X-ray diffraction peaks of *s*-PODO and *i*-PODO establishes that differences in the crystalline morphology may be responsible for the enhanced thermal properties for *s*-PODO.

High molecular weight isotactic and syndiotactic PODO exhibit mechanical and barrier behavior sensitive to processing conditions and crystalline morphology. Highly crystalline stereoregular PODO exhibits exceptionally low oxygen barrier and high modulus. Highly isotactic PODO can be chemically recycled to monomer in high yield, showcasing how tetrahydrofuran-containing polyesters can be promising thermoplastics for a circular economy.

References

1. J.-G. Rosenboom, R. Langer, G. Traverso, Bioplastics for a circular economy. *Nature Reviews Materials* **7**, 117-137 (2022).
2. H. de Beukelaer, M. Hilhorst, Y. Workala, E. Maaskant, W. Post, Overview of the mechanical, thermal and barrier properties of biobased and/or biodegradable thermoplastic materials. *Polymer Testing* **116**, (2022).
3. X. Zhang, M. Fevre, G. O. Jones, R. M. Waymouth, Catalysis as an Enabling Science for Sustainable Polymers. *Chemical Reviews* **118**, 839-885 (2018).
4. G. W. Coates, Y. D. Y. L. Getzler, Chemical recycling to monomer for an ideal, circular polymer economy. *Nature Reviews Materials* **5**, 501-516 (2020).
5. C. Shi, E. C. Quinn, W. T. Diment, E. Y.-X. Chen, Recyclable and (Bio)degradable Polyesters in a Circular Plastics Economy. *Chemical Reviews* **124**, 4393-4478 (2024).
6. M. S. Kim *et al.*, A Review of Biodegradable Plastics: Chemistry, Applications, Properties, and Future Research Needs. *Chemical Reviews* **123**, 9915-9939 (2023).
7. M. J. L. Tschan, R. M. Gauvin, C. M. Thomas, Controlling polymer stereochemistry in ring-opening polymerization: a decade of advances shaping the future of biodegradable polyesters. *Chemical Society Reviews* **50**, 13587-13608 (2021).
8. G. M. Miyake, E. Y.-X. Chen, Cinchona Alkaloids as Stereoselective Organocatalysts for the Partial Kinetic Resolution Polymerization of rac-Lactide. *Macromolecules* **44**, 4116-4124 (2011).
9. M. S. Zaky, A.-L. Wirotius, O. Coulembier, G. Guichard, D. Taton, A chiral thiourea and a phosphazene for fast and stereoselective organocatalytic ring-opening-polymerization of racemic lactide. *Chemical Communications* **57**, 3777-3780 (2021).
10. N. Spassky, M. Wisniewski, C. Pluta, A. Le Borgne, Highly stereoelective polymerization of rac-(D,L)-lactide with a chiral schiff's base/aluminium alkoxide initiator. *Macromolecular Chemistry and Physics* **197**, 2627-2637 (1996).
11. R. Hador, S. Lipstman, R. Rescigno, V. Venditto, M. Kol, Aluminium complexes of salanol ligands: coordination chemistry and stereoselective lactide polymerization. *Chemical Communications* **56**, 13528-13531 (2020).
12. K. Press, I. Goldberg, M. Kol, Mechanistic Insight into the Stereochemical Control of Lactide Polymerization by Salan–Aluminum Catalysts. *Angewandte Chemie International Edition* **54**, 14858-14861 (2015).
13. B. Orhan *et al.*, Isoselective Ring-Opening Polymerization of rac-Lactide from Chiral Takemoto's Organocatalysts: Elucidation of Stereocontrol. *ACS Macro Letters* **7**, 1413-1419 (2018).
14. A. Amgoune, C. M. Thomas, S. Ilinca, T. Roisnel, J.-F. Carpentier, Highly Active, Productive, and Syndiospecific Yttrium Initiators for the Polymerization of Racemic β-Butyrolactone. *Angewandte Chemie International Edition* **45**, 2782-2784 (2006).
15. J. Fang *et al.*, Yttrium catalysts for syndioselective β-butyrolactone polymerization: on the origin of ligand-induced stereoselectivity. *Polym. Chem.* **4**, 360-367 (2013).
16. X. Tang, E. Y.-X. Chen, Chemical synthesis of perfectly isotactic and high melting bacterial poly(3-hydroxybutyrate) from bio-sourced racemic cyclic diolide. *Nature Communications* **9**, 2345 (2018).
17. X. Tang *et al.*, Biodegradable Polyhydroxyalkanoates by Stereoselective Copolymerization of Racemic Diolides: Stereocontrol and Polyolefin-Like Properties. *Angewandte Chemie International Edition* **59**, 7881-7890 (2020).

18. C. G. Jaffredo, Y. Chapurina, S. M. Guillaume, J.-F. Carpentier, From Syndiotactic Homopolymers to Chemically Tunable Alternating Copolymers: Highly Active Yttrium Complexes for Stereoselective Ring-Opening Polymerization of β-Malolactonates. *Angewandte Chemie International Edition* **53**, 2687-2691 (2014).
19. Y. Sun *et al.*, Alternating Sequence Controlled Copolymer Synthesis of α-Hydroxy Acids via Syndioselective Ring-Opening Polymerization of *O* -Carboxyanhydrides Using Zirconium/Hafnium Alkoxide Initiators. *Journal of the American Chemical Society* **139**, 10723-10732 (2017).
20. M. Li *et al.*, Synergetic Organocatalysis for Eliminating Epimerization in Ring-Opening Polymerizations Enables Synthesis of Stereoregular Isotactic Polyester. *Journal of the American Chemical Society* **141**, 281-289 (2019).
21. Q. Feng *et al.*, Stereoselective photoredox ring-opening polymerization of O-carboxyanhydrides. *Nature Communications* **9**, (2018).
22. L. A. H. Sanchez, C. P. Woroch, D. M. Dumas, R. M. Waymouth, M. W. Kanan, Toughening Poly(lactic acid) without Compromise – Statistical Copolymerization with a Bioderived Bicyclic Lactone. *Journal of the American Chemical Society* **147**, 5212-5219 (2025).
23. J. Bruckmoser, S. Remke, B. Rieger, Ring-Opening Polymerization of a Bicyclic Lactone: Polyesters Derived from Norcamphor with Complete Chemical Recyclability. *ACS Macro Letters* **11**, 1162-1166 (2022).
24. Z. Hu *et al.*, Terpenoid-based high-performance polyester with tacticity-independent crystallinity and chemical circularity. *Chem* **10**, 3040-3054 (2024).
25. C. Shi *et al.*, Hybrid monomer design for unifying conflicting polymerizability, recyclability, and performance properties. *Chem* **7**, 670-685 (2021).
26. C. Shi *et al.*, Design principles for intrinsically circular polymers with tunable properties. *Chem* **7**, 2896-2912 (2021).
27. M. Kränzlein *et al.*, Polyester synthesis based on 3-carene as renewable feedstock. *Polymer Chemistry* **13**, 3726-3732 (2022).
28. J.-B. Zhu, E. M. Watson, J. Tang, E. Y.-X. Chen, A synthetic polymer system with repeatable chemical recyclability. *Science* **360**, 398-403 (2018).
29. Y.-T. Li, H.-Y. Yu, W.-B. Li, Y. Liu, X.-B. Lu, Recyclable Polyhydroxyalkanoates via a Regioselective Ring-Opening Polymerization of α,β-Disubstituted β-Lactone Monomers. *Macromolecules* **54**, 4641-4648 (2021).
30. X. Yang *et al.*, Stereoselective Ring-Opening Polymerization of Lactones with a Fused Ring Leading to Semicrystalline Polyesters. *Macromolecules* **55**, 2777-2786 (2022).
31. J.-B. Zhu, E. Y.-X. Chen, Catalyst-Sidearm-Induced Stereoselectivity Switching in Polymerization of a Racemic Lactone for Stereocomplexed Crystalline Polymer with a Circular Life Cycle. *Angewandte Chemie International Edition* **58**, 1178-1182 (2019).
32. J. Zhang *et al.*, Highly Selective O-Phenylene Bisurea Catalysts for ROP: Stabilization of Oxyanion Transition State by a Semiflexible Hydrogen Bond Pocket. *Journal of the American Chemical Society* **146**, 22295-22305 (2024).
33. W. Zhao, F. Cui, J. He, Y. Zhang, E. Y.-X. Chen, Oscillatory adaptive catalysis: Intramolecular chain shuttling regulated by stereo-autocorrection in stereoselective polymerization of lactide. *Chem*, S2451929424003103 (2024).
34. M. J. Stanford, A. P. Dove, Stereocontrolled ring-opening polymerisation of lactide. *Chem. Soc. Rev.* **39**, 486-494 (2010).

35. M. Sebek, J. Holz, A. Börner, K. Jähnisch, Highly Diastereoselective Hydrogenation of Furan-2-carboxylic Acid Derivatives on Heterogeneous Catalysts. *Synlett* **2009**, 461-465 (2009).
36. P. Pino, G. P. Lorenzi, Optically Active Vinyl Polymers. II. The Optical Activity of Isotactic and Block Polymers of Optically Active α-Olefines in Dilute Hydrocarbon Solution. *Journal of the American Chemical Society* **82**, 4455-4467 (1960).
37. Z. Jiang, A. Sen, Palladium(II)-Catalyzed Isospecific Alternating Copolymerization of Aliphatic .alpha.-Olefins with Carbon Monoxide and Isospecific Alternating Isomerization Cooligomerization of a 1,2-Disubstituted Olefin with Carbon Monoxide. Synthesis of Novel, Optically Active, Isotactic 1,4- and 1,5-Polyketones. *Journal of the American Chemical Society* **117**, 4455-4467 (1995).
38. N. Kosaka *et al.*, Conformational Studies on an Optically Active 1,4-Polyketone in Solution. *Macromolecules* **36**, 6884-6887 (2003).
39. H. Y. Huang *et al.*, Access to Polyhydroxyalkanoates with Diverse Syndiotacticity via Polymerization by Spiro-Salen Complexes and Insights into the Stereocontrol Mechanism. *Angewandte Chemie* **137**, (2025).
40. M. Xie *et al.*, Syndioselective Ring-Opening Polymerization of β-Lactones Enabled by Dimethylbiphenyl-Salen Yttrium Complexes. *ACS Macro Letters* **14**, 57-63 (2024).
41. H.-Y. Huang *et al.*, Spiro-salen catalysts enable the chemical synthesis of stereoregular polyhydroxyalkanoates. *Nature Catalysis* **6**, 720-728 (2023).
42. H. Wang, Y. Yang, H. Ma, Stereoselectivity Switch between Zinc and Magnesium Initiators in the Polymerization of rac-Lactide: Different Coordination Chemistry, Different Stereocontrol Mechanisms. *Macromolecules* **47**, 7750-7764 (2014).
43. J. Bruckmoser, S. Pongratz, B. Rieger, High-Throughput Approach in the Ring-Opening Polymerization of β-Butyrolactone Enables Rapid Evaluation of Yttrium Salan Catalysts. *Organometallics* **42**, 876-884 (2023).
44. F. Ding *et al.*, Biomimetic nanocoatings with exceptional mechanical, barrier, and flame-retardant properties from large-scale one-step coassembly. *Science Advances* **3**, (2017).
45. A. Pietrosanto, P. Scarfato, L. Di Maio, M. R. Nobile, L. Incarnato, Evaluation of the Suitability of Poly(Lactide)/Poly(Butylene-Adipate-co-Terephthalate) Blown Films for Chilled and Frozen Food Packaging Applications. *Polymers* **12**, (2020).
46. M. T. Gace *et al.*, Synergistic engineering of poly(3-hydroxybutyrate) architecture and stereomicrostructure achieves enhanced material properties. *Polymer Chemistry* **16**, 4557-4570 (2025).

Acknowledgements: The authors thank Dr. Lucas A. H. Sanchez for helpful discussions, Hannah Bartels for assistance with powder XRD measurements, Louis Diment for assistance with single crystal XRD measurements, Yuran Shi and Alexis Medina for assistance with GPC measurements at Stanford's Soft & Hybrid Materials Facility, Dr. Andro Rios and Dr. David Brook for access to SJSU's polarimeter, and Dr. Steven Lynch for assistance with NMR experiments. The authors also thank Erik G. Rognerud, Dr. Levi J. Hammernik, Sophia Hoffman, and Rose Palmer for assistance with gas barrier, lap shear and tensile measurements and Dr. Gregg T. Beckham and Dr. Nicholas A. Rorrer for access to characterization equipment at the National Laboratories in the Rockies. **Funding:** This work was supported by the National Science Foundation Center for Polymers for a Circular Economy (PCE) (CHE-2317582), the National Science Foundation GOALI Grant (CHE-2002933) and Stanford's Sustainability Accelerator. D.M.D. and K.H.L. acknowledges the Center for Molecular Design (CMAD) for their support. H.Z. acknowledges the Satre Family Stanford Interdisciplinary Graduate Fellowship (SIGF) for their support. Part of this work was supported by the Vincent Coates Foundation Mass Spectrometry Laboratory, Stanford University Mass Spectrometry (RRID:SCR_017801) utilizing the Waters SQD2 LC/MS system (RRID:SCR_022217). Part of this work was performed at nano@stanford RRID:SCR_026695.
Author contributions: R.M.W., M.W.K., and D.M.D. conceived the project and directed research. D.M.D. designed and conducted experiments related to racemic monomer synthesis and polymer characterization. H.Z. designed and conducted experiments related to enantiopure monomer synthesis, homochiral polymer characterization and kinetic modeling of chiral bisurea catalysts. K.H.L. designed and conducted experiments related to catalyst and polymer synthesis. K.H.L., D.M.D., and H.Z. wrote the initial manuscript and revised subsequent versions. All authors contributed to the revised manuscript. **Competing interests:** The authors are named inventors on a provisional US patent application (63/963,679) relating to findings disclosed here. **Data and materials availability:** All data needed to evaluate the conclusions in the paper are present in the paper and/or the supplementary materials.